



## 1D X-RAY SPECKLE PATTERNS: A NOVEL PROBE OF INTERFACIAL DISORDER IN SEMICONDUCTOR SUPERLATTICES

D. L. ABERNATHY<sup>1</sup>, J. ALS-NIELSEN<sup>1</sup>, S. B. DIERKER<sup>2</sup>, R. M. FLEMING<sup>3</sup>,  
G. GRÜBEL<sup>1</sup>, R. PINDAK<sup>3</sup>, K. PLOOG<sup>4</sup> and I. K. ROBINSON<sup>5</sup>

<sup>1</sup>European Synchrotron Radiation Facility, F-38043 Grenoble France

<sup>2</sup>University of Michigan, Ann Arbor, MI 48109, U.S.A.

<sup>3</sup>AT&T Bell Laboratories, Murray Hill, NJ 07974, U.S.A.

<sup>4</sup>Paul-Drude-Institut für Festkörperelektronik, 10117 Berlin, Germany

<sup>5</sup>University of Illinois, Urbana, IL 61801, U.S.A.

**Abstract**—The high brilliance of third generation undulator sources offers an unprecedented opportunity to perform coherent X-ray diffraction studies of the structure and dynamics of materials on length scales down to interatomic spacings. We have measured the coherent diffraction or “speckle” pattern from a GaAs/AlAs superlattice. The speckle diffraction is consistent with height fluctuations of the superlattice of  $\sim 10 \text{ \AA}$  over lengths of order  $60 \mu\text{m}$ . Unlike other methods of characterizing the roughness of semiconductor material, such as scanning probe microscopies (STM, AFM) or scanning electron microscopy (SEM), this novel coherent diffraction method is sensitive to lateral variations of the interface height buried within the small illuminated volume of the material, and thus can offer information unavailable from other non-destructive techniques.

New, brighter, undulator sources of X-rays offer considerable possibilities for altogether different kinds of diffraction experiments. One of these possibilities is to utilize the improved coherence of the beam, which is a quantity associated directly with the source brightness. If a diffraction experiment is carried out with an X-ray beam that is largely coherent, the observed intensity will depend on the relative phases of the scattering of all component parts of the illuminated sample, in addition to all the usual atomic-level structural contributions. In a sample made up of a mosaic of domains, the phases are related to the relative positions of the domains. Much of the excitement in the nascent coherent diffraction, or “speckle”, field[1] stems from the possibility of one day achieving atomic resolution fluctuation spectroscopy: in the case of a sample whose internal domain structure is due to intrinsic fluctuations, such as those associated with a phase transition, the time dependence of the fluctuations may be probed by monitoring the variations in intensity of the coherent diffraction signal.

Coherent diffraction of X-rays is a new subject, with relatively little published work to date. One significant previous study[2] investigated the static grain structure induced in a sample of  $\text{Cu}_3\text{Au}$  by quenching from above its disordering temperature. In other static work, speckle has been recorded from a structured polymer thin film[3]. Recently experimental time-correlation functions have been observed in two systems,  $\text{Fe}_3\text{Al}$  near to its critical temperature[4], and in small-angle scattering from colloidal gold[5].

Historically, temporal effects have been discussed mainly in the context of coherent light scattering, where the time structure of a scattered signal can be readily interpreted in terms of diffusion or motions of scattering objects[6]. The information so-obtained is always on a length scale of the wavelength of light, and so the traditional technique is inherently unable to probe contrast on an atomic scale. X-rays offer the appealing possibility of extending these powerful techniques to probe motions on the scale of individual atoms.

Here we investigate the practicality of interpreting the static coherent diffraction from a simple structure, an artificial semiconductor multilayer prepared by molecular beam epitaxy (MBE). We first describe our measurements, which were made during an experimental run that utilized undulator radiation for coherent diffraction for the first time, at the European Synchrotron Radiation Facility (ESRF) in Grenoble. These data can be understood at a quantitative level, by constructing a random phase model in which the illuminated part of the sample is considered to be a phase structure made up of discrete scattering blocks, each with its own phase relative to its neighbors[7]. This method can in principle give information about the static height fluctuations or roughness of buried interfaces in layered semiconductor materials.

The measurements were made at the ID10 “Troika” beamline[8] at ESRF in which the radiation source is a permanent magnet undulator. The beam was monochromated with a single-bounce sideways-scattering water-cooled thin Si(220) crystal located

45 m from the source and set to an energy of 12 keV ( $\lambda = 1.05 \text{ \AA}$ ). The thin crystal passed a significant fraction of the power of the beam to assist the cooling[9]. The total incident power was reduced further by closing horizontal slits at the 27 m point of the beamline. Harmonics in the diffracted beam from the monochromator were filtered by reflection from a SiC mirror which restored the beam to the horizontal plane. The sample was located at 46 m, mounted on a four-circle diffractometer, oriented with its principal axis vertical.

One critical parameter in a coherent diffraction experiment is the lateral (or transverse) coherence length. A perfectly monochromatic plane wave has a constant phase everywhere in a plane perpendicular to its wavevector  $\mathbf{k}$ . Two monochromatic plane waves propagating in directions differing by an angle  $\Delta\theta$  will have a phase difference of  $2\pi$  within this plane at a distance  $\xi_{\perp}$ , the lateral coherence length, given by  $(k\Delta\theta)\xi_{\perp} = 2\pi$ .  $\Delta\theta$  is determined by the finite size of the X-ray source, which is either intrinsic to the storage ring or may be set by a slit or pinhole inserted into the beam. If a source of size  $w$  is located at a distance  $W$  from the point of observation, then  $\Delta\theta = w/W$ , and  $\xi_{\perp} = (2\pi/k)\Delta\theta = \lambda W/w$ . The intrinsic undulator source width at ID10 is not isotropic, but has  $w_H = 1026 \mu\text{m}$  (FWHM) in the horizontal and  $w_V = 225 \mu\text{m}$  (FWHM) in the vertical directions. We therefore made use of the horizontal slit at  $W_1 = 19 \text{ m}$ , set to an opening of  $w_1 = 100 \mu\text{m}$ , to satisfy  $W_1/w_1 = W/w_V$ , to obtain an approximately isotropic lateral coherence length of  $\xi_{\perp} = 21 \mu\text{m}$  at the sample position,  $W = 46 \text{ m}$ .

The longitudinal coherence length,  $\xi_{\parallel}$ , is determined solely by the bandwidth of the monochromator,  $\xi_{\parallel} = \lambda/(\Delta E/E)$ . For a symmetric Si(220) reflection at 12 keV,  $\Delta E/E$  is estimated to be  $5.1 \times 10^{-5}$ , giving  $\xi_{\parallel} = 2 \mu\text{m}$ . The longitudinal coher-

ence must be longer than the maximum path-length difference (PLD) in the experiment, in order to observe the coherent effects. In our experiment, which uses the symmetrical extended-face geometry, the PLD is  $\mu^{-1} \sin 2\theta_B$ , where  $\mu^{-1}$  is the absorption length and  $\theta_B$  is the Bragg angle of diffraction.  $\mu^{-1}$  is estimated to be  $28.7 \mu\text{m}$  and  $\theta_B = 0.79^\circ$  for the sample and measurements described here, giving a PLD of only  $0.006 \mu\text{m}$ . From this we conclude that the longitudinal coherence is sufficiently good that it can be ignored.

To select a coherent beam for the experiment, it is necessary to place an aperture in front of the sample with an opening smaller than  $\xi_{\perp} = 21 \mu\text{m}$ . We used a nominal  $d_1 = 7 \mu\text{m}$  circular aperture ("pinhole") laser-drilled into a  $50 \mu\text{m}$  Pt sheet, centered behind a  $0.5 \text{ mm}$  hole drilled in a  $1 \text{ mm}$  thick Ta plate. This pinhole was mounted on a precision X-Y stage with submicron repeatability. This front pinhole was located approximately  $100 \text{ mm}$  before the sample, at the center of the four-circle goniometer. A second, back pinhole of diameter  $d_2 = 20 \mu\text{m}$  or  $d_2 = 5 \mu\text{m}$  was installed on the  $2\theta$ -arm of the diffractometer at a distance  $D = 1.3 \text{ m}$  from the sample, and followed by a scintillator/photomultiplier detector. The experimental layout is sketched in Fig. 1. The MBE-grown sample consisted of 377 repetitions of alternating layers of GaAs and AlAs on a GaAs(100) substrate. The period was 13.5 layers or  $38 \text{ \AA}$ .

The coherence of a beam is usually measured as its fringe visibility or contrast[10]. In order to observe this, scans were made of the direct beam without a sample. One example is shown in Fig. 2(a), for pinhole diameters  $d_1 = 7 \mu\text{m}$  and  $d_2 = 5 \mu\text{m}$ . The data are presented as counting rate vs back pinhole position,  $y$ . We denote the direction parallel to the motion of the diffractometer's  $2\theta$ -arm as  $y_{\parallel}$  (horizontal in our setup) and the perpendicular direction as  $y_{\perp}$

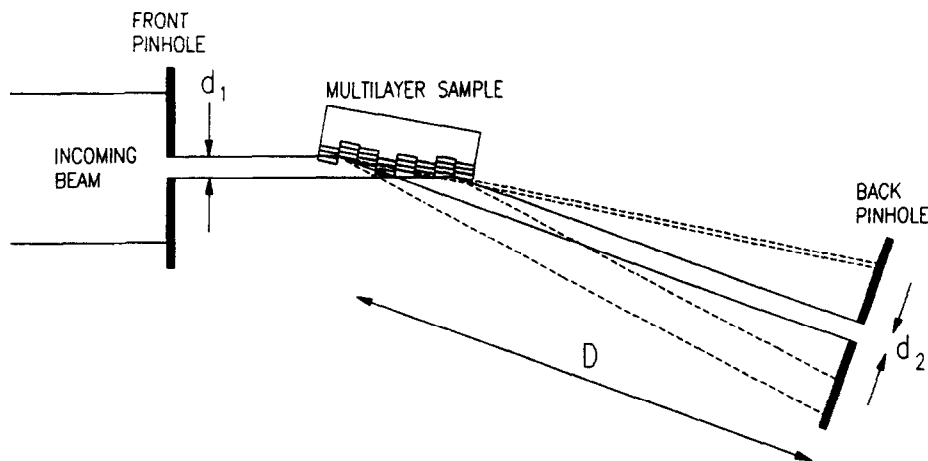


Fig. 1. Layout of the experiment. The front pinhole selects a part of the monochromatized undulator X-ray beam that is essentially phase coherent across its size  $d_1$ . This illuminates the multilayer sample at the Bragg angle for one of the superlattice reflections. The microscopic "block" structure assumed in the model is drawn exaggerated for clarity. The angular distribution of the scattering is measured by a scintillation detector behind a pinhole of size  $d_2$  at a distance  $D$  from the sample.

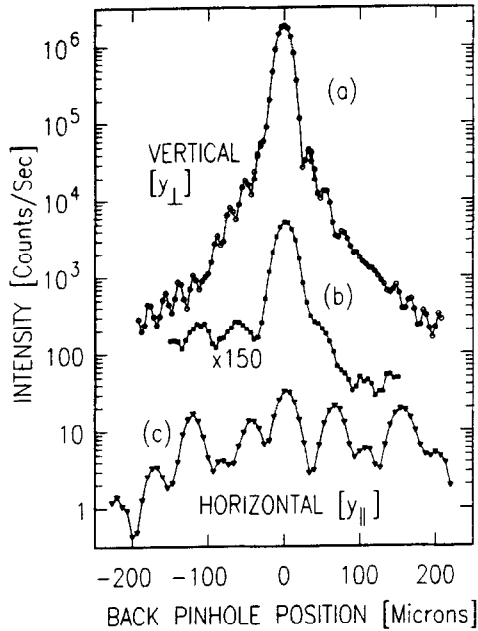


Fig. 2. (a) Measurement of the Fraunhofer diffraction from a  $d_1 = 7 \mu\text{m}$  front pinhole analyzed by a  $d_2 = 5 \mu\text{m}$  back pinhole scanned in the vertical direction. (b) Coherent diffraction of the  $(000)^+$  peak from the multilayer sample along the vertical direction. A  $7 \mu\text{m}$  front and a  $20 \mu\text{m}$  back pinhole were used. Note that the central peak has the same width as the Fraunhofer diffraction in (a). (c) Coherent diffraction of the same peak as (b) along the horizontal direction using the same pinhole configuration. Several peaks are observed, with each peak having roughly the width of the Fraunhofer diffraction in (a).

(vertical in our setup). Fringes are seen with different contrast in the direction examined ( $y_{\perp}$ ). This type of behavior was also observed in other directions, as well as for the other pinholes tested. The non-ideal intensity distribution is believed to be a property of the precise shape of the pinhole, and the straightness of its edges.

The sample was then installed and aligned on the first-order diffraction of the superlattice. Following the usual convention, this peak is a satellite of the origin of reciprocal space, and so it is denoted  $(000)^+$ . The diffraction coming from the sample was analyzed in the two directions  $y_{\perp}$  and  $y_{\parallel}$ , and is shown in Fig. 2(b) and (c), respectively. The  $y_{\perp}$  scan shows a single peak 20 times more intense than the background features, with the same width as the direct beam in Fig. 2(a). The  $y_{\parallel}$  scan shown in Fig. 2(c) is totally different, and shows many peaks within a broad envelope function. The individual peaks each have approximately the  $55 \mu\text{m}$  minimum-to-minimum width of the corresponding scan across the direct beam in Fig. 2(a), which has about the width expected for the circular Fraunhofer diffraction from the nominally around  $d_1 = 7 \mu\text{m}$  source pinhole itself,  $1.22 \times 2\lambda D/d_1 = 51 \mu\text{m}$ , minimum-to-minimum[10].

The distribution of peaks in Fig. 2(c) is the "speckle" pattern. An experimental verification that

this depends sensitively on the fine structure of the sample is shown in Fig. 3. The only difference between curves (a) and (b) in Fig. 3 is that the front and back pinholes were shifted perpendicular to the scattering plane by  $20 \mu\text{m}$  in the  $y_{\perp}$  direction (out of the plane of the page in Fig. 1) to illuminate a different part of the sample. Although its qualitative features, e.g. the overall width, are preserved the heights and positions of all the peaks are substantially changed between the two patterns.

The dramatic difference between scans (b) and (c) of Fig. 2 shows that the speckle pattern is one-dimensional with significant speckle features in the  $2\theta$  ( $y_{\parallel}$ ) direction only. At first glance this result is enigmatic, since there is nothing anisotropic about the fabrication of the sample, which should be cylindrically symmetric. In conventional diffraction experiments, a peak broadening in the  $2\theta$  direction is interpreted as due to variations of lattice parameter, just as the perpendicular directions correspond to mosaic spread. It is of course perfectly reasonable that an artificial multilayer sample should have intrinsic  $d$ -spacing disorder, but it turns out that this is irrelevant to the interpretation of the speckle, except to the extent that it changes the ultimate position of the outermost layers.

We note that the Bragg angle of the  $(000)^+$  superlattice reflection,  $\theta_B$ , is only  $0.79^\circ$ . This grazing angle of incidence onto the multilayer has two important consequences.

Since the absorption length of 12 keV X-rays in GaAlAs is  $\mu^{-1} = 28.7 \mu\text{m}$ , the penetration depth of the beam into the sample at this angle is  $t = \frac{1}{2}\mu^{-1}/\sin$

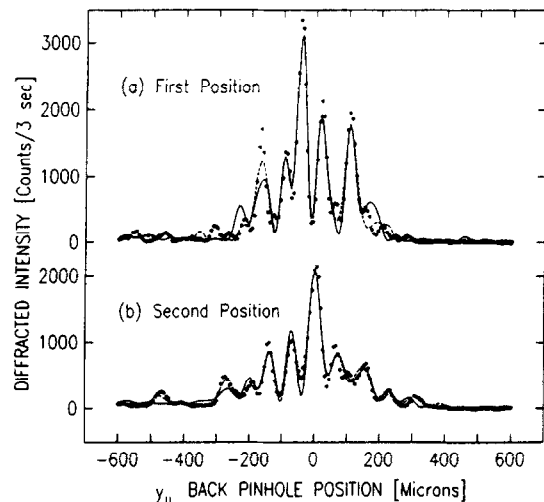


Fig. 3. Intensity distribution of the speckle patterns recorded for the  $(000)^+$  superlattice peak of the  $38 \text{ \AA}$ -period GaAs/AlAs multilayer, as a function of the back pinhole position,  $y_{\parallel}$ , measured in the scattering plane along the direction of the Bragg angle. The two sets of data (a) and (b) correspond to two different positions on the sample separated by  $20 \mu\text{m}$  in the lateral position (perpendicular to the page in Fig. 1). Curves are calculated from the model briefly described in the text.

$\theta_B$ , or only  $0.20 \mu\text{m}$ , considerably smaller than the width of the coherent beam emerging from the front pinhole ( $d_1 = 7 \mu\text{m}$ ). The coherent diffraction effects observed in Fig. 2(c) therefore cannot come from variations of the phase of scatterers along the depth direction. Instead, since the size of the illuminated spot on the sample is  $d_1/\sin \theta_B = 500 \mu\text{m}$  in the horizontal and  $d_z = 7 \mu\text{m}$  in the vertical, we conclude that the necessary interference must arise from scatterers spread out in the lateral directions instead. The grossly elongated "footprint" explains the apparent anisotropy between  $y_1$  and  $y_\perp$ [7].

Comparing Fig. 2(a,b,c), we see that the size of each speckle peak is the same as the Fraunhofer central maximum. This is a necessary consequence of the fact that a small region of the sample is illuminated, and all diffraction is broadened by that finite size. The envelope of all the peaks is considerably broader, however, and this must be inversely related to the finite size of each coherently-scattering grain in the sample. For this reason, we can see that there is a general relationship between the total number of speckle peaks (here about eight) and the number of grains in the sample. This number roughly corresponds to the number of phases of interfering waves needed to construct the speckle pattern as an interference sum. The effective grain size is hence of order  $500 \mu\text{m}/8 \approx 60 \mu\text{m}$ . This lateral grain dimension is therefore larger than the beam in the transverse direction, which explains why no substantial speckle was seen in the  $y_\perp$  direction.

Thus, we conclude that the phase variations necessary to produce the observed speckle must be due to lateral variations of scattering phase. This is illustrated schematically by the "block" structure drawn on the sample in Fig. 1. The block represents the extent of a region of the sample that scatters with a single phase; adjacent blocks have distinct phase differences between them. The argument given above may be generalized to say that any variations of the internal vertical structure of the blocks (such as  $d$ -spacing disorder) cannot be the origin of the phase difference, because such structure will always give rise to features that are very broad ( $\sim 2\pi/t$ ) along the surface normal direction. To accrue a phase shift of the order of  $\pi$  between adjacent blocks, it is necessary to have a height difference between their outermost diffracting planes of half a superlattice period, or  $19 \text{ \AA}$ , which seems to be reasonable over a lateral distance of  $60 \mu\text{m}$  for the variation of film thickness out of total of  $15,000 \text{ \AA}$  grown. Since we estimated there were of order eight clear speckles in the pattern, we conclude there must be of order eight such distinct blocks within the footprint of the coherent beam.

Assuming this block model of the sample then allows us to construct a functional description of the speckle. The diffraction from each block is assumed to be perfectly specular, and to differ from that of its neighbors only by an arbitrary phase associated with the local height of the multilayer modulations above

the substrate. When illuminated by a perfectly coherent X-ray beam the sample may be considered to be a linear phase array emitting wavefronts with a different phase from each block. If  $x$  represents the position across the beam, which extends over the range  $0 < x < d_1$  at the sample position, then the phase of the diffracted beam can be approximated by a discrete value corresponding to each of the  $N$  blocks.

$$\phi(x) = \phi_j \quad (j-1)d_1/N < x < jd_1/N \quad j = 1, \dots, N. \quad (1)$$

If we observe the superposition of the wavefronts on a screen a large distance  $D$  from the sample, then the amplitude variation with position on the screen  $y$  is found from the standard Fraunhofer integral[11] to be

$$A(y) = \frac{\sin(\pi d_1 y / N \lambda D)}{\pi y / \lambda D} \times \sum_{j=1}^N \exp \left( 2\pi i \left( j - \frac{1}{2} \right) \frac{d_1 y}{N \lambda D} + i\phi_j \right). \quad (2)$$

Thus the diffraction pattern is seen to be the product of a wide  $\sin(x)/x$  slit function with a width corresponding to the block size, multiplied by a complex "random phase sum" over the block phases  $\phi_j$ . This random phase sum modulates the amplitude within the envelope of the block slit function, thereby providing the two length scales seen in our speckle patterns: the width of the fine structure (individual speckles) arising from the size of the beam and the envelope width coming from the size of the blocks. The penetration depth is too small to contribute.

The screen in the discussion above is, of course, the position of our back pinhole (see Fig. 1), or of a film or position-sensitive detector in other experiments. Thus the observed intensity through this second pinhole is just the square modulus of eqn (2) convolved with a box function the size of the pinhole. In our case the back pinhole was  $d_2 = 20 \mu\text{m}$  at a distance of  $D = 1.3 \text{ m}$ ; this is sufficiently small that the convolution represents only a negligible correction to the widths. The square modulus of eqn (2) was therefore used to compare directly with the data.

Several ways of fitting the model described by eqn (2) to the observed speckle patterns of Fig. 3 have been tested[7]. In brief, because of the large number of parameters with no *a priori* information to limit their values, alternating cycles of least-squared refinements and systematic or random (Monte-Carlo) searches of parameter space were employed. When the number of scattering blocks was held to  $N = 8$ , it was possible to reasonably exhaust all possible combinations of phases. The resulting model intensities are plotted as lines in Fig. 3. Fits were also performed with  $N$  as large as 17, but no definitive statements about a global minimization can be made. One interesting feature of these fits, however, was the systematic occurrence of sudden jumps in the phases between regions of slow variation. One may speculate

that these locations, which were reproduced by different fits, are growth defects in the multilayer structure that may arise from instabilities such as step-bunching during growth[12].

Several significant conclusions about the understanding of speckle patterns have arisen from this study. First, even when a symmetric beam is used, strongly anisotropic speckle can result from the use of a grazing geometry. Second, when the penetration depth is much smaller than the lateral dimensions of the coherently diffracting domains, the vertical structure of the sample becomes unimportant, because its effects become smeared out by the finite-size broadening due to the limited penetration. The relevant phase of the domain is then determined only by the relative position of the diffracting planes at the surface. Finally, the fine details of the speckle patterns observed can be understood by a random phase model, for which practical methods of solving for the values of a limited set of phases are being developed.

We do not believe this is necessarily a unique description of speckle, but instead a working model that embodies some of its important characteristics. It invites further testing of more powerful ways of gaining information about the microscopic arrangement of the domains within a small region of a sample. For example, if two speckle patterns were recorded before and after a sample displacement by less than the size of the beam's footprint, they would be related in a way that might allow phasing of the peripheral material. A sequence of difference measurements might then allow a complete phase map to be generated experimentally.

We note in closing that the technique described here may have some practical utility in non-destructive roughness determination of semiconductor materials on an important length scale. The typical distances probed are also accessible to optical interferometry, scanning probe microscopies (STM and AFM) or scanning electron microscopy (SEM). The coherent diffraction method differs from all of these others, however, in that it probes the lateral variation in height of a diffracting layer inside the material, which is not necessarily related to its surface. In the case of a semiconductor heterostructure device, for example used as a quantum-well, it is the roughness of the interfaces that determines the electron scattering, hence mobility, and this is precisely the roughness to which the diffraction method is sensitive. The coherent diffraction experiment differs from recent advances in understanding the diffuse, non-

specular X-ray scattering from rough multilayers[13], in that it can be considered a local probe of the detailed structure of the system instead of a statistical evaluation of the roughness averaged over large areas of the sample. With further advances the information available from coherent X-ray scattering may be of use in evaluating layered semiconductor structures.

*Acknowledgements*—We thank the staff of the ESRF, particularly P. Feder and H. Gleyzolle, for valuable assistance and hospitality during execution of the experiment. We were greatly assisted in the setting up of the experiment by G. B. Stephenson, S. Brauer, S. G. J. Mochrie and M. Sutton. I.K.R. and S.B.D. acknowledge support from the U.S. National Science Foundation under grants DMR93-15691 and DMR92-17956.

#### REFERENCES

1. G. Grübel, J. Als-Nielsen, D. Abernathy, G. Vignaud, S. Brauer, G. B. Stephenson, S. G. J. Mochrie, M. Sutton, I. K. Robinson, R. Fleming, R. Pindak, S. Dierker and J. F. Legrand, *ESRF Newslett.* **20**, 14 (1994); G. Grübel, D. Abernathy, G. B. Stephenson, S. Brauer, I. McNulty, S. G. J. Mochrie, B. McClain, A. Sandy, M. Sutton, E. Dufresne, I. K. Robinson, R. Fleming, R. Pindak and S. Dierker, *ESRF Newslett.* **23**, 14 (1995).
2. M. Sutton, S. G. J. Mochrie, T. Greytak, S. E. Nagler, L. E. Berman, G. A. Held and G. B. Stephenson, *Nature* **352**, 608 (1991).
3. Z. H. Cai, B. Lai, W. B. Yun, I. McNulty, K. G. Huang and T. P. Russel, *Phys. Rev. Lett.* **73**, 82 (1994).
4. S. Brauer, G. B. Stephenson, M. Sutton, R. Brüning, E. Dufresne, S. G. J. Mochrie, G. Grübel, J. Als-Nielsen and D. L. Abernathy, *Phys. Rev. Lett.* **74**, 2010 (1995).
5. S. B. Dierker, R. Pindak, R. M. Fleming, I. K. Robinson and L. Berman, *Phys. Rev. Lett.* **75**, 449 (1995).
6. B. Chu, *Laser Light Scattering: Basic Principles and Practices*. Academic Press, San Diego (1991).
7. I. K. Robinson, R. Pindak, R. M. Fleming, S. B. Dierker, K. Ploog, G. Grübel, D. L. Abernathy and J. Als-Nielsen, *Phys. Rev. B* **52**, 9917 (1995).
8. G. Grübel, J. Als-Nielsen and A. K. Freund, *J. Phys. IV* **4**, C9-27 (1994).
9. J. Als-Nielsen, A. K. Freund, G. Grübel, J. Linderholm, M. Nielsen, M. Sanchez del Rio and J. P. F. Sellschop, *Rev. Sci. Instrum.* **B94**, 306 (1995).
10. J. W. Goodman, *Statistical Optics*. Wiley, New York (1985).
11. J. M. Cowley, *Diffraction Physics*. North Holland, Amsterdam (1975).
12. M. D. Johnson, C. Orme, A. W. Hunt, D. Graff, J. Sudijono, L. M. Sander and B. G. Orr, *Phys. Rev. Lett.* **72**, 116 (1994).
13. V. Holý and T. Baumbach, *Phys. Rev. B* **49**, 10,668 (1994); T. Salditt, T. H. Metzger and J. Peisl, *Phys. Rev. Lett.* **73**, 16 (1995); J.-P. Schlomka, M. Tolan, L. Schwalowsky, O. H. Seeck, J. Stettner, and W. Press, *Phys. Rev. B* **51**, 2311 (1995).